Molecular Biology, Vol. 30, No. 6, Part 2, pp. 812–817, 1996

Molecular Dynamics and Electron-Conformational Interactions in Ferredoxin

N. K. Balabaev,[1] A. S. Lemak,[1] and K. V. Shaitan[2]

UDC 577.322

Translated from *Molekulyarnaya Biologiya*, Vol. 30, No. 6, pp. 1348-1356, November-December, 1996.

Original article submitted February 16, 1996.

Numerical modeling of the molecular dynamics of *Peptococcus aerogenes* ferredoxin at 300°K in different charge states of iron–sulfur clusters revealed a decrease as well as an increase in the mean distance between clusters upon protein reduction, despite that the electrostatic repulsion between them increased markedly. To describe the low-frequency protein motions on the basis of the molecular-dynamic paths obtained, use was made of a quasiharmonic model. The vibration spectrum for the oxidized protein was composed of two characteristic frequency bands, 1–90 and 120–200 cm^{-1}. The low-frequency spectrum was virtually insensitive to the Fe/S cluster charge state. The protein was shown to significantly affect the average structure of the $Fe_4S_4(SH)_4$ complex, altering both its symmetry and the interatomic distances. The largest displacements were found for SH groups (0.4 Å). The deviations of the Fe_4S_4 atoms from equilibrium structure were about 0.07 Å, and the change in the Fe–S bond length was insignificant (<0.005 Å).

Key words: computing experiment; conformational relaxation; quasiharmonic analysis

Computer modeling of molecular dynamics (MD) is regarded as a source of important information on the processes taking place in biological macromolecules and complexes thereof. In the chemical aspect, the functioning of the living organism is based on redox reactions. A central part therein is played by the electron transfer chain proteins, which act as electron carriers in some important biochemical reactions. Understanding how the organic milieu controls the redox processes is of fundamental importance [1–4]. Recent attempts at solving this problem involved numerical MD modeling of the photosynthetic reaction center (RC) [5–9]. The latter is a complicated protein array embedded in a lipid membrane. The abundant experimental material available provides an opportunity for a theoretical study of the processes taking place in protein complexes. In particular, the data testify to the great importance of the protein response to charge separation in the RC [10]. At the same time, the RC appears to be a very complicated object for a theoretical consideration of microscopic processes.

At the present stage, we chose the protein ferredoxin (Fd) as an object for examining the processes associated with the changes in the electronic state of the redox center. This protein is found in anaerobic bacteria and plays a key part in enzymic metabolism and nitrogen fixation. On the other hand, analysis of the Fd sequence and structure shows that this protein appeared early in evolution. Thus it could be hoped that Fd would show a pronounced enough response to a change in its electronic state. Preliminary results on Fd dynamics have been published elsewhere [11].

MODELED OBJECT

The protein under study belongs to the group of bacterial ferredoxins of like physicochemical properties and functions. These small (~6000 Da) water-soluble proteins transfer two electrons at a quite low redox potential, ~400 mV.

The 3D structure of *Peptococcus aerogenes* Fd has been established [12, 13]. The protein comprises 54 amino acid residues and two iron–sulfur clusters Fe_4S_4 (in total, 389 heavy atoms). Figure 1 displays the main chain course and the position of clusters. Fd is shaped as an ellipsoid of rotation with 22 × 27 Å dimensions. Each cluster is attached to the protein matrix by four chemical bonds between its irons and the sulfurs of

[1]Institute of Mathematical Problems in Biology, Russian Academy of Sciences, Pushchino, Moscow Region, 142292.
[2]Lomonosov State University, Moscow, 119899.

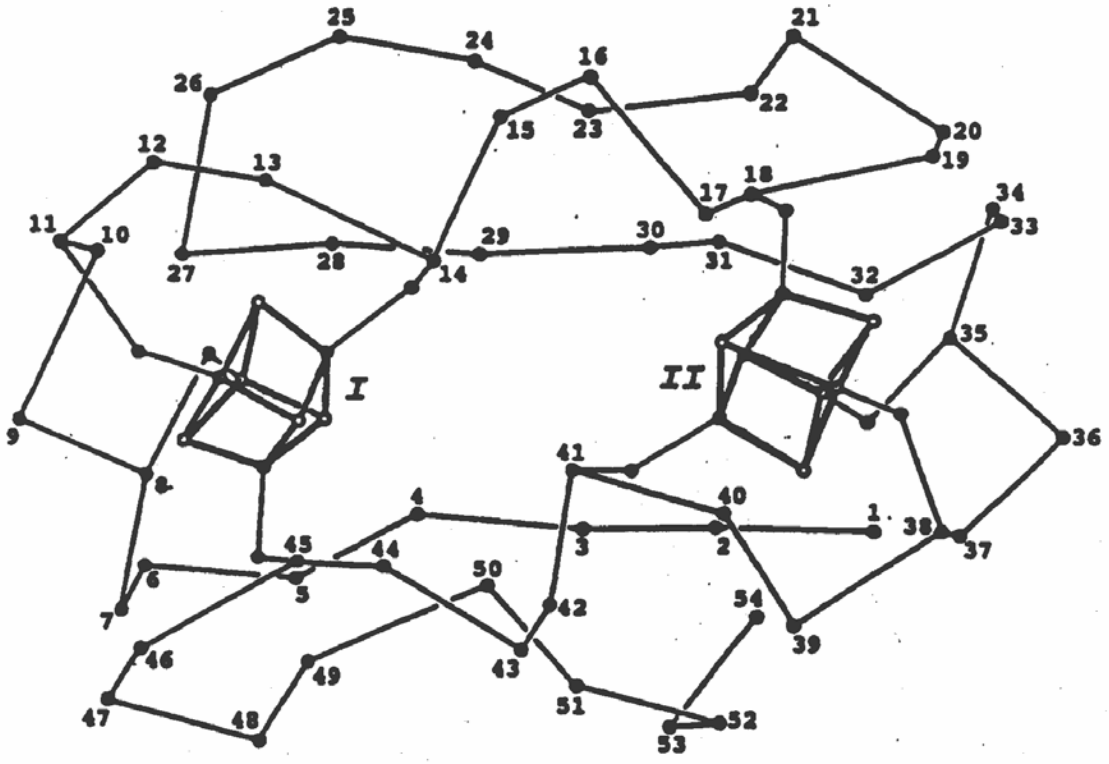

Fig. 1. Positions of C_α atoms and all atoms of two $Fe_4S_4(S_\gamma)_4$ complexes in the X-ray structure of ferredoxin [6].

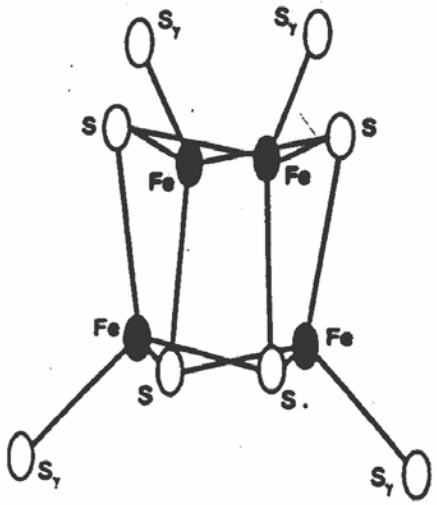

Fig. 2. Equilibrium structure of the $Fe_4S_4(S_\gamma)_4$ complex (according to Table 2).

cysteine residues 8, 11, 14, 45 for cluster 1 and 18, 35, 38, 41 for cluster 2. The spatial arrangement of the eight atoms of one cluster and the four bound cysteine sulfurs is shown in Fig. 2. Fd is almost devoid of aromatic residues.

COMPUTATIONAL DETAILS

Standard MD techniques [14, 15] were applied to oxidized and reduced Fd, using a heavy-atom model and the method of Berendsen et al. [16] at constant temperature. The potential energy $U(r)$ determining the force field has components corresponding to deformations of valence bonds and angles, torsion angles, van der Waals and Coulomb noncovalent interactions, and H-bonding. The force interaction parameters and partial charges on the polypeptide chain atoms were taken from [17]. To account for solvent shielding, the polar amino acids on the protein surface were assumed to be neutral; to allow for high-frequency polarization of the milieu, the dielectric constant was taken to be $\varepsilon = \varepsilon_\infty = 2$. Electrostatic interactions were calculated for all pairs of charged atoms regardless of the distance between them; van der Waals interactions were considered only for pairs of atoms spaced by no more than 9 Å.

The interaction parameters for Fe/S cluster atoms absent from [17] were chosen on the basis of our quantum-mechanical calculations and literature data [18–20]. Partial charges on cluster atoms were derived from X-alpha computations for model compounds [18]; the partial charges for both forms are given in Table 1. Note that the sum charge of the $Fe_4S_4(S_\gamma)_4$ complex is -2e in the oxidized and -3e in the reduced state. Both states were assumed to have the same equilibrium geometry and force field parameters of the clusters. The equilibrium values used in calculations are listed in Table 2. The force constants were obtained by quantum-mechanical calculations for $Fe_4S_4(S_\gamma)_4H_4$ using the CNDO-S^2 method [21].

The X-ray structure of oxidized Fd [13] from the protein database was taken as the initial one; the initial rates were set at random. Preliminarily, the protein structure had been relaxed by a standard procedure

TABLE 1. Partial Charges on $Fe_4S_4(S_\gamma)_4$ Atoms

Atom	Charge, e	
	Ox	Red
Fe	−0.05	−0.10
S	−0.27	−0.37
S_γ	−0.18	−0.28

TABLE 2. Valent Interaction Parameters for $Fe_4S_4(S_\gamma)_4$

Bond or angle	Length (Å) or angle (deg)	Force constant, kcal·mole^{-1}Å^{-2}, kcal·mole^{-1}rad^{-2}
Fe—S	2.288	143
Fe—S_γ	2.25	201
Fe—S—Fe	73.74	32.5
S—Fe—S	104.12	25.4
S_γ—Fe—S	114.37	25.4
Fe—S_γ—C2	103.0	50.0

[14, 15] at constant temperature T_0 = 300°K. The duration of this relaxation stage was 80 psec. Then two MD paths of 100 psec at 300°K were obtained for the oxidized and reduced states. The integration step was 1 fsec, the characteristic time of interaction with the thermostat τ_T = 1 psec.

QUASIHARMONIC MODEL

To describe the low-frequency modes of protein movement, including residue collective motions as a whole, each of the 54 residues was represented as a separate interaction center (quasiatom) coinciding in position with C_α. Both Fe/S clusters were also represented as separate quasiatoms situated at the cluster centers of mass.

The internal coordinates of the system were introduced by setting virtual bonds between quasiatoms along the protein chain [22, 23]. These were supplemented with a bond connecting the clusters and a bond connecting one cluster to Cys45. The internal coordinates q defining the conformation of the model system were then naturally plotted according to the virtual bonds along the chain. In total, there were 162 internal coordinates: 55 virtual bonds, 54 virtual valence angles, and 53 virtual torsion angles.

In a quasiharmonic approximation [23–25] the potential energy is a quadratic function of the selected internal coordinates, i.e., the effective Lagrangian appears as

$$L_{eff} = \frac{1}{2}\sum_{i,k=1}^{162} H_{ik}\dot{q}^i\dot{q}^k - \frac{1}{2}\sum_{i,k=1}^{162} F_{ik}(q^i - q_0^i)(q^k - q_0^k).$$

where q are internal coordinates, q_0 are their equilibrium values, H_{ik} are kinetic energy matrix elements, F_{ik} are effective force constants. The latter three values are obtained by MD calculation for the protein at temperature T: q_0 are the mean q values along the MD path; H_{ik} are computed at point q_0; the force constant matrix F is unequivocally connected with the covariation matrix of q fluctuations:

$$F = k_B T \cdot S^{-1},$$

where the elements of matrix S are found by averaging the products

$$S_{ik} = \langle (q^i - q_0^i)(q^k - q_0^k) \rangle .$$

along the MD path.

With the resulting quasiharmonic model, for an ensemble of dynamic systems defined by L_{eff} the Gibbs averages of q^i and products thereof for all i and k coincide with the corresponding means derived along the protein MD path. This, in its turn, gives grounds for believing that the other characteristics obtained for this linear dynamic system correctly reflect the dynamic properties of the protein molecule. The Lagrangian was processed routinely to determine the intrinsic vectors and frequencies identified with the low-frequency modes of protein motion.

RESULTS

Low-frequency protein motions. The frequency distributions for a simplified protein model in the quasiharmonic approximation for oxidized and reduced Fd are shown in Fig. 3. In both cases there are two characteristic bands, 1–90 and 120–190 cm^{-1}. The

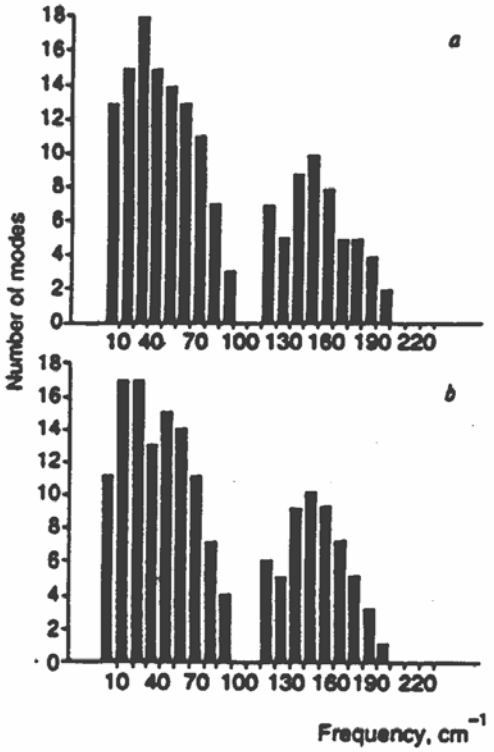

Fig. 3. Frequency distributions derived from the Fd quasiharmonic model in oxidized (*a*) and reduced (*b*) states.

low-frequency maximum corresponds to collective motions of protein structural units, which interact rather weakly through the van der Waals potential. The high frequencies correspond to localized stretching of virtual bonds and angles. The frequency spectra are practically the same in reduced and oxidized states, except for the twofold difference in the minimal frequencies (respectively 1.37 and 0.70 cm^{-1}).

Distance between clusters. The temporal behavior of the distance R between the Fe/S clusters in Fd is of special interest as regards the processes of electron transfer and the general theory of electron-conformational interactions in biopolymers. A most intriguing question is whether $R(t)$ would be an isolated mode in protein motion. Analysis of the normal modes obtained in the quasiharmonic approximation indicates that there is no mode where R is the only variable. The relative changes in R upon a shift along each mode by the equilibrium amplitude are shown in Fig. 4. As can be seen, there are quite a few modes noticeably changing the R. Maximal fluctuations, 0.16 Å, are observed in the 9.76 cm^{-1} mode; this amounts to ~45% of the rms fluctuation σ_R in the distance between clusters along the MD path (σ_R = 0.352 Å). In about 10 modes, the R fluctuations are about 0.08 Å, i.e., 20% of σ_R. Hence $R(t)$ is not an isolated mode, and the clusters are engaged in collective movements of the protein matrix.

Structural relaxation during Fd reduction. The engagement of clusters in collective protein motions may result in nontrivial behavior of the intercluster distance with time. Of special interest is the decrease in R during MD modeling, observed upon instantaneous reduction of protein in certain conformational space regions.

In the oxidized state, each cluster has a charge of -2e, which causes strong electrostatic repulsion between them. Protein polarization induced by cluster charges together with the stress in the protein matrix fully compensate for this repulsion. When the protein is reduced, the charge on one cluster increases to -3e. Though this further enhances the repulsion between clusters, the distance decreases from R_{ox} = 13.8 to R_{red} = 13.2 Å. Protein reduction entails conformational rearrangements whereby the rise in energy caused by cluster approach is counterbalanced by the decrease in the energy of cluster interaction with protein polarization (see Table 3). Shortening of the distance should increase the rate of electron exchange between clusters, which appears functionally important.

It should, however, be emphasized that protein reduction in other conformational space regions may also cause an increase in the mean intercluster distance. The regions were varied by choosing the initial reduction point at different moments on the MD path pertaining to the oxidized state. It is important that the corresponding relaxed states persisted for at least 100 psec (duration of the simulation). On the other hand, these data point to the multiple pathways of protein relaxation on the potential energy hypersurface [26].

Average structure of the $Fe_4S_4(SH)_4$ complex. One of the possible approaches to assessing the specific influence of the protein environment on the structure of the $Fe_4S_4(SH)_4$ complex is to compare the behavior of the complex in the protein and in a generalized medium acting as an energy reservoir (thermostat). To this end, the method of collision dynamics [27] was applied to the complex at 300°K. In the calculations, the potential energy included only valent interactions with parameters as in Table 2. The mean rate of collisions with the surrounding molecules per atom was set at λ = 2 $psec^{-1}$. At this value, the energy

TABLE 3. Components of Electrostatic Energy (kcal/mole)

Interaction	Oxidized state	During reduction	Reduced state
Protein–protein	−148	−148	−148
Protein–cluster	−98	−123	−130
Cluster–cluster	48	72	76

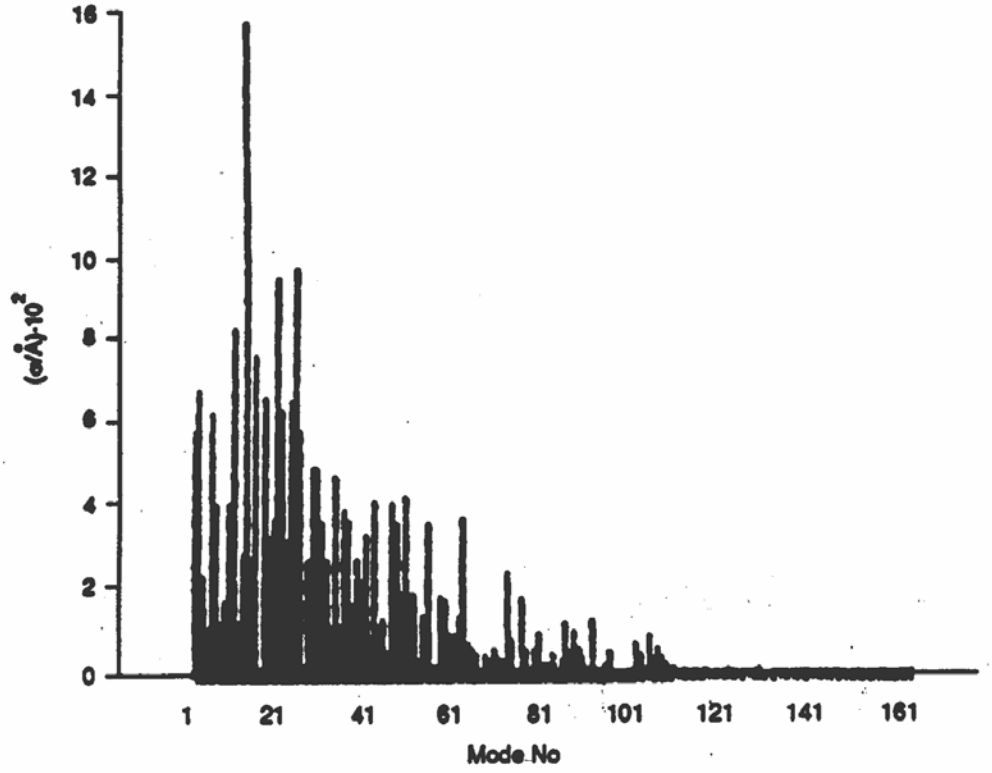

Fig. 4. Contribution of quasiharmonic vibration modes to rms fluctuations in the distance between Fe/S clusters in Fd.

exchange between the complex and the collision medium was similar to that in Fd [27].

Further we shall compare the behavior of the complex along three paths: those for complexes 1 and 2 isolated from the MD path of oxidized Fd, and one in collision medium. Therewith we can define three average structures, designated respectively as C1, C2, and C3, and compare them with the equilibrium (unstressed) structure C0. The latter is formed of three tetrahedrons containing respectively Fe, inorganic S, and cysteine S_γ at their apices. The tetrahedrons are regular, with edges Fe–Fe of 2.746 Å, S–S of 3.609 Å, and S_γ–S_γ of 6.419 Å. They are arranged in space so that their centers of mass coincide, all Fe–S bonds are 2.288 Å, and all Fe–S_γ bonds are 2.25 Å (Fig. 2).

Table 4 lists the interatomic distances in C1–C3. As can be seen, C3 differs somewhat from the equilibrium structure; deviations of Fe–S, Fe–Fe, and S–S are within 0.5%, and those of Fe–S_γ and S_γ–S_γ are within 1.5%. In structures C1 and C2, the respective deviations from equilibrium values are within 1% for Fe–S, 3.5% for Fe–Fe, S–S, and Fe–S_γ, and reach 11% for S_γ–S_γ. The tetrahedron edges are deformed by less than 0.1 Å in Fe–Fe and S–S, and by 0.6 Å in S_γ–S_γ. The centers of mass of the Fe and S tetrahedrons coincide, while that of S_γ is shifted by 0.13 Å. Note that the deviations of C1 and C2 from C0 are less than the rms fluctuations of atoms along the paths considered: σ = 0.15 Å for cluster atoms and σ = 0.36 Å for organic sulfur in all three cases.

A quantitative measure of the deviation of an average structure from equilibrium may be the complex deformation energy. The latter consists of the deformation energies for valence bonds and angles in accordance with Table 2. As follows from Table 5, the valence angles in C3 are practically not deformed,

TABLE 4. Interatomic Distances in Average $Fe_4S_4(SH)_4$ Complex Structures

Bond	Cluster 1 in protein		Cluster 2 in protein		Cluster in collision medium	
	b, Å	Δb, Å	b, Å	Δb, Å	b, Å	Δb, Å
Fe—Fe	2.713	0.076	2.717	0.09	2.738	0.003
S—S	3.593	0.094	3.589	0.104	3.597	0.003
S_γ—S_γ	6.277	0.604	6.309	0.441	6.362	0.019
Fe—S	2.273	0.009	2.272	0.009	2.280	0.001
Fe—S_γ	2.202	0.017	2.213	0.011	2.22	0.001

Note. b) Mean length over all bonds of given type in complex; Δb) maximal deviation from the mean.

TABLE 5. Deformation Energy for Average $Fe_4S_4(SH)_4$ Complex Structures

E_{def}, kcal/mole	Cluster 1 in protein		Cluster 2 in protein		Cluster in collision medium	
E_1	3.537	100	2.572	100	0.410	100
E_2	1.188	33.6	0.766	29.8	0.408	99.5
E_3	0.789	22.3	0.648	25.2	0.068	16.6
E_4	0.213	6.0	0.213	8.3	0.068	16.6

Note. Deformation energies for E_1) whole $Fe_4S_4(SH)_4$ complex, E_2) valence bonds in complex, E_3) total Fe_4S_4 cluster, E_4) valence bonds in cluster; asterisked values are percentages of E_1.

indicating that C3 retains the C0 symmetry; therewith the interatomic distances decrease by some 0.01 Å. In C1 and C2 (clusters in Fd) the deformation is an order of magnitude greater, with both the symmetry and the interatomic distances altered. The largest displacements are found for S_γ, whereas the deformation of the Fe_4S_4 cluster proper accounts for only 25% of the overall deformation of the complex; the least deformed are the Fe–S bonds (only 6% of the total deformation).

Ferredoxin is a relatively small protein; nonetheless, it practically isolates the two Fe_4S_4 clusters from the solvent, holding them about 12 Å apart. The eight cysteine residues in the polypeptide chain are arranged so as to ensure definite spatial positioning and structure of the clusters. As follows from the results of this work, the polypeptide chain forms with the clusters a unified dynamic system giving a collective response to electron transfer. Therewith the molecule relaxation is not invariant, and depends on the details of the macromolecular configuration at the moment of altering the charge state of reacting groups. This creates physical premises for using the effects of electron-conformational interactions in regulation of protein function [26].

The work was supported by the Russian Foundation for Basic Research (95-04-12197a) and the Siberian Trade Bank.

REFERENCES

1. M. V. Vol'kenshtein, *Biophysics* [in Russian], Nauka, Moscow (1988).
2. L. A. Blyumenfel'd, *Problems of Biological Physics* [in Russian], Nauka, Moscow (1977).
3. A. B. Rubin, *Biophysics* [in Russian], Vysshaya Shkola, Moscow, Vol. 1 (1987).
4. K. V. Shaitan, *Mol. Biol.*, 26, 264–284 (1992).
5. H. Treutlein, K. Schulten, J. Deisenhofer, H. Michel, A. Brunger, and M. Karplus, In: J. Breton and A. Vermeglio (editors), *The Photosynthetic Bacterial Reaction Center*, Plenum, N. Y. (1988), pp. 139–150.
6. S. Creighton, J.-K. Hwang, A. Warshel, W. W. Parson, and M. Karplus, *Biochemistry*, 27, 774–781 (1988).
7. A. Warshel, Z. T. Chu, and W. W. Parson, *Science*, 246, 112–116 (1989).
8. M. Nonella and K. Schulten, *J. Phys. Chem.*, 95, 2059–2067 (1991).
9. K. Schulten and M. Tesch, *Chem. Phys.*, 158, 421–446 (1991).
10. K. V. Shaitan, I. V. Uporov, E. P. Lukashev, A. A. Kononenko, and A. B. Rubin, *Mol. Biol.*, 25, 695–705 (1991).
11. N. K. Balabaev and A. S. Lemak, *Proc. SPIE*, 1921, 375–385 (1993).
12. E. T. Adman, L. C. Sieker, and L. H. Jensen, *J. Biol. Chem.*, 248, 3987–3996 (1973).
13. E. T. Adman, L. C. Sieker, and L. H. Jensen, *J. Biol. Chem.*, 251, 3801–3806 (1976).
14. J. A. McCammon and S. C. Harvey, *Dynamics of Proteins and Nucleic Acids*, Cambridge Univ. Press (1987).
15. Ch. L. Brooks III, M. Karplus, and B. M. Pettitt, *Proteins: A Theoretical Perspective of Dynamics, Structure, and Thermodynamics*, John Wiley & Sons, N. Y. (1987).
16. H. J. C. Berendsen, J. P. M. Postma, W. F. VanGunsteren, A. Dinola, and J. R. Haak, *J. Chem. Phys.*, 81, 3684–3690 (1984).
17. B. Gelin and M. Karplus, *Biochemistry*, 18, 1256–1268 (1979).
18. L. Noodleman, J. G. Norman, J. H. Osborne, A. Aizman, and D. A. Case, *J. Am. Chem. Soc.*, 107, 3418–3426 (1985).
19. A. Aizman and D. A. Case, *J. Am. Chem. Soc.*, 104, 3269–3279 (1982).
20. R. S. Czernuszewicz, K. A. Macor, M. K. Johnson, A. Gewirth, and T. G. Spiro, *J. Am. Chem. Soc.*, 109, 7178–7187 (1987).
21. M. J. Filatov, O. V. Gritsenko, and G. M. Zhidomirov, *Theor. Chim. Acta*, 72, 211 (1987).
22. D. A. Brant and P. J. Flory, *J. Am. Chem. Soc.*, 87, 2791–2800 (1965).
23. R. M. Levy, A. R. Srinivasan, and W. K. Olson, *Biopolymers*, 23, 1099–1112 (1984).
24. R. M. Levy, O. L. Rojas, and R. A. Friesner, *J. Phys. Chem.*, 88, 4233–4238 (1984).
25. M. Karplus and J. N. Kushick, *Macromolecules*, 14, 325–332 (1981).
26. K. V. Shaitan, *Mol. Biol.*, 28, 670–678 (1994).
27. A. S. Lemak and N. K. Balabaev, *Molecular Simulation*, 13, 177–187 (1994).